International Journal of Microwave and Wireless Technologies, 2015, 7(3/4), 239–249.
doi:10.1017/S1759078715000069

RESEARCH PAPER

Evaluation of coaxial cable performance under thermal gradients

SERGIO COLANGELI, RICCARDO CLERITI, WALTER CICCOGNANI AND ERNESTO LIMITI

This paper presents a very flexible tool for numerically evaluating the small-signal and noise parameters of a transmission line subject to an arbitrary thermal gradient. Contrary to previous methods, the proposed approach allows straightforwardly taking into account possible variations of electrical parameters along the propagation direction, such as may be expected when temperature ranges between very different values. The main application of the proposed method is cable modeling in noise-figure measurement setups under cryogenic operation: in such circumstances, indeed, the coaxial cables (or waveguide) at the interface between the outside and the inside of the cryogenic chamber are subject to remarkable temperature excursions. As a consequence, significant de-embedding errors may arise if the cables are not correctly modeled, given the very low values of noise figure which are commonly exhibited by cryo-cooled active devices.

Keywords: Linear and non-linear CAD techniques, Passive components and circuits

Received 13 October 2014; Revised 23 December 2014; Accepted 04 January 2015; first published online 30 March 2015

I. INTRODUCTION

Cryogenic cooling represents one of the most promising concepts to obtain ultra-low-noise amplifiers (LNAs), especially if combined with advanced III–V hetero-structure technologies, such as InP HEMTs [1, 2]. Possible applications of cryo-cooled LNAs are in radio astronomy, satellite communication, and mobile base stations [3–5]. Small-signal and noise characterization of cryo-cooled active devices, however, requires very specific instrumentation – in particular, cryogenic probe stations – and is in general a critical operation by itself. Moreover, owing to the extremely low-noise figures, which are common in this kind of measurements, great care should be taken to minimize every possible source of uncertainty: in this regard, the very techniques adopted for characterization and modeling may affect the final results [1, 6–11].

As well known, one such source of uncertainty lies in the de-embedding process [12], through which the noise contribution of the auxiliary components in the measurement chain has to be removed. In typical ambient-temperature noise measurements, these components are passive and at thermal equilibrium, so that their noise behavior is easily determined based on their small-signal parameters. Unfortunately, however, this approach is no longer valid when dealing with the coaxial cables which connect the outside and the inside of the cryogenic chamber: these cables are subject to a remarkable temperature excursion, and the hypothesis of thermal equilibrium must be removed. The aim of this contribution is to investigate the effects of significant thermal gradients on the small-signal and noise parameters of a coaxial cable such as those used in typical cryogenic probe stations. This topic has not been explored very much in the literature, the only noteworthy references being [13] and, from a different standpoint [14].

The remainder of this paper is structured as follows: Section II presents the key observation that of non-uniform physical temperature in a generic two-port network prevents one from easily deriving the two-port's noise parameters from its small-signal parameters. Section III illustrates a first solution to the problem, for the more specific case in which the two-port is a transmission line and temperature variations only take place along the direction of signal propagation; in Section IV the proposed numerical approach is simplified on the basis of typically valid assumptions. Then, Section V points up a possible way to obtain the small-signal parameters necessary to apply the general-purpose and simplified approaches. The different techniques presented so far are briefly summarized in Section V, to provide the Reader with a comprehensive, yet synthetic overview. Section VII reports some experimental results to validate the proposed formulation. The main conclusions of this work are summarized in Section VIII.

II. GENERAL FRAMEWORK

It is well known that the equivalent noise temperature, T_{eq}, of a passive two-port at thermal equilibrium can be derived from the two-port's physical temperature, T_{ph}, and available gain, G_{av}:

$$T_{eq} = T_{ph} \cdot \left(\frac{1}{G_{av}} - 1 \right). \quad (1)$$

Department of Electronic Engineering, University of Rome Tor Vergata, via del Politecnico 1, 00133 Rome, Italy. Phone: +39 7259 7343
Corresponding author:
S. Colangeli
Email: colangeli@ing.uniroma2.it

Note that, whereas T_{eq} and G_{av} depend on the source reflection coefficient of the two-port, Γ_S, T_{ph} is constant.

Friis' formula, here recalled:

$$T_{eq} = T_{ph,1} + \frac{T_{eq,2}}{G_{av,1}} + \frac{T_{eq,3}}{G_{av,1}G_{av,2}} + \cdots \tag{2}$$

can be used to derive the equivalent noise temperature of a pair of such two-ports, at different physical temperatures:

$$\begin{aligned} T_{eq,12} &= T_{ph,1} \cdot \left(\frac{1}{G_{av,1}} - 1\right) + T_{ph,2} \cdot \left(\frac{1}{G_{av,2}} - 1\right) \cdot \frac{1}{G_{av,1}} \\ &= (T_{ph,1} - T_{ph,2}) \cdot \left(\frac{1}{G_{av,1}} - 1\right) + T_{ph,2} \cdot \left(\frac{1}{G_{av,1}G_{av,2}} - 1\right). \end{aligned} \tag{3}$$

It is clear that (3) cannot be recast in the form of (1), that is, no constant "effective" temperature, $T_{ph,eff,12}$, exists such that $T_{eq,12}$ can be expressed as $T_{ph,eff,12} \cdot (1/\mathrm{Gav},12 - 1$ for all source reflection coefficients, where $G_{av,12} = G_{av,1} \cdot G_{av,2}$ – unless in trivial cases, such as if $T_{ph,2} - T_{ph,1} = 0$, or if at least one of the two-ports is lossless. With respect to the latter example, note that for a lossless two-port the physical temperature is not uniquely defined (i.e., any physical temperature would equally yield the parameters of a noiseless two-port).

Equation (3) also hints that temperature differences along a chain of passive two-ports act as weighting functions in a summation of terms, so that, in general, the optimum noise match is not simply the reflection coefficient which maximizes the available gain of a particular two-port of the chain. On the other hand, in the particular case in which the component two-ports all exhibit the same optimum source match with respect to the available gain, that termination would also yield the optimum noise match of the whole chain.

III. GENERAL-PURPOSE NUMERICAL APPROACH

Different numerical approaches may be devised to address the computation of the noise factor of a uniform transmission line subject to a thermal gradient. In the following, one such methodology is presented, which resembles the approach described in [13], although applied in a sensibly more convenient way: in particular, a completely algebraic formulation has been developed, not relying on a circuit simulator.

The key point of this numerical approach consists in discretizing the problem – that is, the original transmission line is split into a large number, n, of smaller segments: if n is large enough, each segment may be considered as subject to a constant physical temperature, and therefore exhibiting well-defined small-signal and noise parameters. As a consequence, by suitably combining these parameters (which is straightforward) it is possible to approximate the solution to the original problem with arbitrary accuracy.

Telegrapher's equations provide an intuitive representation of transmission lines, as depicted in Fig. 1(a), in terms of four real (possibly frequency-dependent) parameters, R, L, G, and C, representing the resistance, inductance, conductance, and capacitance, respectively, per unit length of line. More

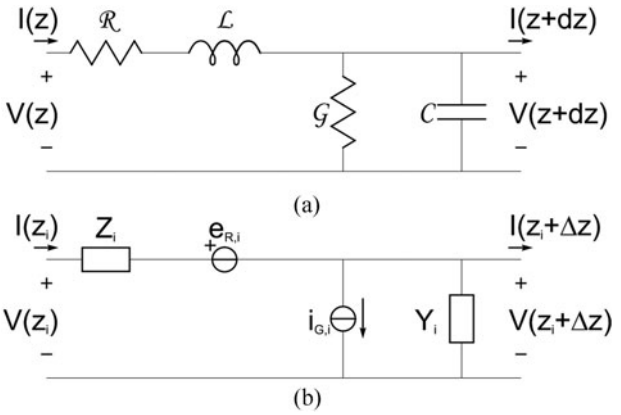

Fig. 1. Telegrapher's representation of an elementary section of transmission line. (a) Infinitesimal cell. (b) Discrete cell, with noise sources.

synthetically, an impedance, Z, and an admittance, Y, per unit length can be defined at any angular frequency ω, as follows:

$$Z = R + j\omega L, \tag{4}$$

$$Y = G + j\omega C. \tag{5}$$

From these so-called "primary parameters," the secondary parameters of the transmission line are derived, namely the characteristic impedance:

$$Z_c = \sqrt{\frac{R + j\omega L}{G + j\omega C}} = \sqrt{\frac{Z}{Y}} = R_c + jX_c, \tag{6}$$

and the propagation constant:

$$\gamma = \sqrt{(R + j\omega L) \cdot (G + j\omega C)} = \sqrt{Z \cdot Y} = \alpha + j\beta \tag{7}$$

with α the attenuation constant (Np/m) and β the phase constant (rad/m). Note that, apart from uninteresting cases (DC frequency or lossless line), the characteristic impedance is never purely real; nevertheless, it may safely be considered such in coaxial cables for high-frequency operation (from a few hundred megahertz up).

Whereas the representation of Fig. 1(a) is only exact in the limit for infinite sections of infinitesimal length, dz, a transmission line can be approximated by the cascade of a large number of short cells of finite length, Δz. The ith finite-length cell of the cascade will be made up of a series impedance and a parallel admittance given, respectively, by:

$$Z_i = R_i + j\omega L_i = Z \cdot \Delta z, \tag{8}$$

$$Y_i = G_i + j\omega C_i = Y \cdot \Delta z, \tag{9}$$

where the cells are numbered from $i = 0$ to $i = n - 1$, so that each of them is enclosed between $z_i = i \cdot \Delta z$ and $z_{i+1} = z_i + \Delta z = (i + 1) \cdot \Delta z$.

The real parts of immittances Z_i and Y_i can be associated with noise generation. In particular, this noise is represented in Fig. 1(b) by a series voltage source $e_{R,i}$ and a parallel

https://doi.org/10.1017/S1759078715000069 Published online by Cambridge University Press

current source $i_{G,i}$, of values such that:

$$\overline{|e_{R,i}|^2} = 4kBT_{ph,i}R_i,\ s, \tag{10}$$

$$\overline{|i_{G,i}|^2} = 4kBT_{ph,i}G_i, \tag{11}$$

where $T_{ph,i}$ is the physical temperature of the cell. More specifically, $T_{ph,i}$ approximates the physical temperature along the transmission line, $T_{ph}(z)$, as follows:

$$T_{ph,i} \cong T_{ph}(z_i) = T_{ph}(i \cdot \Delta z). \tag{12}$$

Note that the hypothesis of zero correlation between $e_{R,i}$ and $i_{G,i}$, that is:

$$\overline{e_{R,i}i^*_{G,i}} = 0 \tag{13}$$

is in agreement with the results which would be obtained in the case of constant temperature, for which (1) can be applied. This assumption is also made, implicitly, in [13], where fundamentally the same approach is used, although in a more complicated fashion. As a last comment in this respect, zero correlation can be justified by the fact that the microscopic noise sources associated with the metal (therefore to R_i) and those associated with the dielectric (therefore to G_i) are spatially separated.

According to Hillbrand and Russer's noise correlation matrix formulation [15, 16], the chain representation of the noise correlation matrix of the ith cell, $\mathbf{C}_i$, can be computed as:

$$\begin{aligned}\mathbf{C}_i &= \begin{bmatrix} \overline{|e_{n,i}|^2} & \overline{e_{n,i}i^*_{n,i}} \\ \overline{e^*_{n,i}i_{n,i}} & \overline{|i_{n,i}|^2} \end{bmatrix} \\ &= \begin{bmatrix} 1 & Z_i \\ 0 & 1 \end{bmatrix} \cdot \begin{bmatrix} \overline{|e_{R,i}|^2} & \overline{e_{R,i}i^*_{G,i}} \\ \overline{e^*_{R,i}i_{G,i}} & \overline{|i_{G,i}|^2} \end{bmatrix} \cdot \begin{bmatrix} 1 & Z_i \\ 0 & 1 \end{bmatrix}^H, \\ &= \begin{bmatrix} \overline{|e_{R,i}|^2} + |Z_i|^2 \cdot \overline{|i_{G,i}|^2} & 0 \\ 0 & \overline{|i_{G,i}|^2} \end{bmatrix},\end{aligned} \tag{14}$$

where superscript H denotes the conjugate transpose matrix and the last equivalence exploited hypothesis (13). Moreover, the ith cell is associated with an ABCD matrix, $\mathbf{A}_i$:

$$\mathbf{A}_i = \begin{bmatrix} 1 + Z_iY_i & Z_i \\ Y_i & 1 \end{bmatrix}. \tag{15}$$

It can be shown that the correlation matrix of the cascade including all cells along the transmission line is equal to:

$$\mathbf{C} = \mathbf{C}_o + \sum_{i=1}^{n-1} \left(\prod_{k=0}^{i-1} \mathbf{A}_k \right) \cdot \mathbf{C}_i \cdot \left(\prod_{k=0}^{i-1} \mathbf{A}_k \right)^H. \tag{16}$$

In deriving (16), the noise contribution of each cell has been shifted leftwards, based on the small-signal parameters of the cable portion preceding it (namely, the cascade of cells from $k = 0$ to $k = i - 1$).

Note that, even if frequency is fixed in the above discussion, the four primary parameters may still depend on the physical temperature of the transmission line. Moreover, if the physical temperature varies along the longitudinal direction, the primary parameters will also be functions of z, as implicitly assumed with retaining subscripts in equations (8)–(16). The formulation presented in this section is, therefore, well suited to take into account the possible dependency of the electrical parameters on temperature. If, on the other hand, this dependency is negligible, then all cells exhibit the same small-signal behavior, so that (16) simplifies to:

$$\mathbf{C} = \mathbf{C}_o + \sum_{i=1}^{n-1} \mathbf{A}^i_o \cdot \mathbf{C}_i \cdot (\mathbf{A}^i_o)^H. \tag{17}$$

Equations (16) and (17) allow us to evaluate numerically the correlation matrix of a transmission line subject to an arbitrary thermal gradient: note that, since the terms of the input matrices are functions of $T_{ph,i}$, this must be preliminary determined for all values of i. In a second step, the standard noise parameters of the transmission line can be computed with well-known conversion formulae [6, 12]:

$$\begin{cases} R_n = \hat{c}_{11}, \\ Y_{opt} = \sqrt{\dfrac{\hat{c}_{22}}{\hat{c}_{11}} - \left(\dfrac{\Im\{\hat{c}_{12}\}}{\hat{c}_{11}} \right)^2} + j\dfrac{\Im\{\hat{c}_{12}\}}{\hat{c}_{11}}, \\ F_{min} = 1 + 2(\hat{c}_{12} + \hat{c}_{11}Y^*_{opt}), \end{cases} \tag{18}$$

where the generic $\hat{c}_{lm}$ represents term (l, m) of $\mathbf{C}$, normalized on k_BBT_o. Here k_B is the Boltzmann's constant, B the considered bandwidth (customarily, 1 Hz), and T_o is the standard noise temperature (i.e., 290 K).

IV. SIMPLIFIED NUMERICAL APPROACH

The numerical approach presented in Section III can be applied virtually to any transmission line, since it manages arbitrary shapes of temperature and electrical parameters. Moreover, it offers the possibility of associating different temperatures with the metal- and dielectric-related lossy elements, should this feature be judged important in some circumstances. Nevertheless, this generality is paid with an often unnecessary complexity of implementation. In addition, that approach requires a significant computation time, since for the algorithm to converge to an accurate result a very large number of cells per length has to be chosen, even with moderate temperature excursions: this is due to the necessity of emulating the distributed behavior of a transmission line, independent of the temperature shape.

Such intricacies can usually be avoided by simplifying the problem at its very root. The first step in doing so, and arguably the one which best of all still keeps the solution at a very general validity, is restricting the discussion to small-loss transmission lines. Under this assumption, it is well known that a line's characteristic impedance is independent of R and G, but it is set exclusively by L and C:

$$Z_c \cong \sqrt{\frac{L}{C}}, \tag{19}$$

so that perturbations of R and G do not affect Z_c, which can be considered a real-valued constant throughout along the line.

https://doi.org/10.1017/S1759078715000069 Published online by Cambridge University Press

As to γ, a first-order expansion leads to the following approximation:

$$\gamma \cong \frac{\sqrt{L \cdot C}}{2} \cdot \left(\frac{R}{L} + \frac{G}{C}\right) + j\omega\sqrt{L \cdot C}, \tag{20}$$

from which it is clear that the imaginary part of the propagation constant does not depend on line losses, while only its real part does.

For the moment, let α be constant along z, so that the scattering transmission matrix of the transmission line can be expressed as:

$$\begin{aligned}\mathbf{T} &= \begin{bmatrix} e^{-\gamma l} & 0 \\ 0 & e^{+\gamma l} \end{bmatrix} = \begin{bmatrix} e^{-\alpha l} & 0 \\ 0 & e^{+\alpha l} \end{bmatrix} \cdot \begin{bmatrix} e^{-j\beta l} & 0 \\ 0 & e^{+j\beta l} \end{bmatrix} \\ &= \mathbf{M} \cdot \mathbf{P}, \end{aligned} \tag{21}$$

where the normalization impedance Z_0 has been set real and equal to Z_c, and two auxiliary matrices have been defined:

$$\mathbf{M} = \begin{bmatrix} e^{-\alpha l} & 0 \\ 0 & e^{+\alpha l} \end{bmatrix}, \tag{22}$$

$$\mathbf{P} = \begin{bmatrix} e^{-j\beta l} & 0 \\ 0 & e^{+j\beta l} \end{bmatrix}. \tag{23}$$

After choosing a suitable value of n, the scattering transmission matrix of the ith cell are computed from those of the full length of transmission line. In particular, the scattering transmission matrix of the ith cell can again be factored as the product of two diagonal matrices: $\mathbf{M}_i$, accounting for magnitude variations, and $\mathbf{P}_i$, accounting for phase variations.

In this discretized formulation, it is straightforward to get back the (possible) dependence of α on z:

$$\begin{aligned}\mathbf{M}_i &= \begin{bmatrix} e^{-\alpha_i l} & 0 \\ 0 & e^{+\alpha_i l} \end{bmatrix} = (\mathbf{M}_u)^{k_i} = \begin{bmatrix} e^{-\alpha_u l} & 0 \\ 0 & e^{+\alpha_u l} \end{bmatrix}^{k_i} \\ &= (\mathbf{M}^{1/n})^{k_i} = \begin{bmatrix} e^{-\alpha_u l/n} & 0 \\ 0 & e^{+\alpha_u l/n} \end{bmatrix}^{k_i} \forall i \in \{0, 1, 2, \ldots, n-1\}, \end{aligned} \tag{24}$$

while β cannot vary in the hypothesis of small losses:

$$\begin{aligned}\mathbf{P}_i &= \begin{bmatrix} e^{-\beta_i l} & 0 \\ 0 & e^{+\beta_i l} \end{bmatrix} = \mathbf{P}_u = \begin{bmatrix} e^{-\beta_u l} & 0 \\ 0 & e^{+\beta_u l} \end{bmatrix} \\ &= \mathbf{P}^{1/n} = \begin{bmatrix} e^{-\beta_u l/n} & 0 \\ 0 & e^{+\beta_u l/n} \end{bmatrix} \quad \forall i \in \{0, 1, 2, \ldots, n-1\}. \end{aligned} \tag{25}$$

Subscript u in (24) and (25) represents the nominal cell parameters, i.e. those of any cell in the case of a uniform transmission line, whereas $k_i = \alpha_i/\alpha_u$ plays the role of weighing cell losses with respect to the uniform case (for which it would be $k_i = 1 \forall i$). In particular, it is easily verified that the average of all k_i is always unit by definition. In conclusion, the parameters of the ith cell are:

$$\begin{aligned}\mathbf{T}_i &= \mathbf{M}_i \cdot \mathbf{P}_i = (\mathbf{M}_u)^{k_i} \cdot \mathbf{P}_u = (\mathbf{M}^{1/n})^{k_i} \cdot \mathbf{P}^{1/n}, \\ &\forall i \in \{0, 1, 2, \ldots, n-1\}, \end{aligned} \tag{26}$$

which can be easily computed from the knowledge of the overall scattering transmission matrix and a parameter k_i, which is a function of the discrete steps z_i. Once the temperature and small-signal parameters of each cell are known, matrices $\mathbf{A}_i$ and $\mathbf{C}_i$ of Section III are easily derived, and (16) can be applied, so as to obtain the full set of noise parameters.

It is worth noting that, with respect to the approach described in Section III, only one real parameter (k_i) needs to be computed versus the longitudinal axis rather than four (R_i, L_i, G_i, and C_i) – or possibly two (R_i and G_i). Beside this, several advantages come with this simplified approach:

- implementing the algorithm is significantly more straightforward;
- this algorithm naturally lends itself to manage measured S-parameters of transmission lines, in addition to simulated, ideal parameters.

The latter issue is very valuable when one needs to know the small-signal behavior of a physical transmission line – such as a coaxial cable – subject to a thermal gradient. In the similar situations, the desired information can be derived from scattering measurements at ambient temperature, which are simple to carry out, plus numerical simulations concerning thermal shape and line losses. On the contrary, directly measuring cable parameters under cryogenic conditions may be time consuming, unless coaxial standards can be mechanically switched. In addition, the simulation-based approach can also provide the noise parameters of the cable under test with a marginal extra effort.

To illustrate this, notice that the small-signal parameters of a real cable can be directly inserted in (26), as long as it is well matched (or at least symmetric, in which case the original S-parameters can be renormalized to obtain $S_{11} = S_{22} = 0$ at each frequency). A benefit of this procedure is that, as the thermal excursion is reduced, the S-parameters elaborated on the basis of (26) will approach the original parameters as temperature approaches the (constant) ambient value – which would not be the case for a purely simulation-based approach. Similar considerations hold for noise parameters derived by exploiting (26).

As a further simplification, it is possible to also take advantage of some empirical results exemplified in Fig. 2: by comparing the measured S-parameters of a coaxial cable subject to a significant temperature excursion (150°C) to those of the same cable at ambient temperature it can be observed that the only significant variations are in $|S_{12}|$. Therefore, the S-parameters of the cable under thermal gradients can be approximated by those at ambient temperature, provided that transmission parameters are corrected in magnitude based on computed k_i: as shown in the bottom axis of Fig. 2, $|S_{12}|$ measurements under thermal excursion are almost undistinguishable from the elaboration of $|S_{12}|$ at ambient temperature.

Finally, a comparison is presented in Fig. 3 between the general-purpose approach of Section III and the simplified approach of the current section to show that the latter converges to accurate values much faster. Since the two

https://doi.org/10.1017/S1759078715000069 Published online by Cambridge University Press

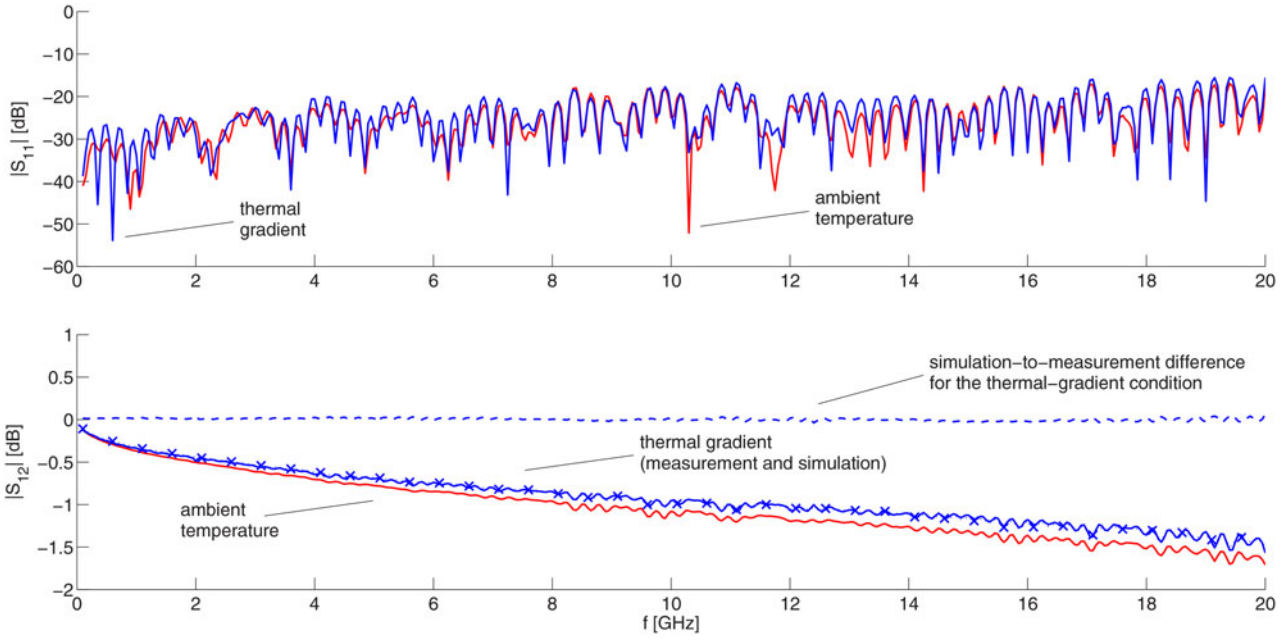

Fig. 2. Sample measured *S*-parameters in magnitude of a coaxial cable at ambient temperature and under a 150°C thermal excursion. Measurements are carried out by the unterminating method. In the bottom, axis are also shown (cross-markers) the magnitude of *S*12 under thermal excursion as derived from *S*12 at ambient temperature through the approach described in Section IV, as well as (dashed line) the difference between measured and estimated magnitude of *S*12. Normalization impedance is 50 Ω.

methods are based on different formulations, to get a meaningful comparison two sets of equivalent parameters had to be chosen, as reported in Table 1. Note that with the general-purpose approach a characteristic impedance very close to $Z_o = 50\ \Omega$ is obtained at the selected frequency, and that in both cases the available gain on 50 Ω is about 3 dB. The noise factor plotted, F_n, is referred to a mismatched source termination, namely $|\Gamma_S| = 0.75$, and the subscript n denotes the number of cells used for the numerical evaluation.

Of course, in case no thermal gradients were present, the general-purpose approach would still need a considerable number of cells to converge, whereas the simplified approach would give the exact result for any n. The reason for this difference lies in the fact that, with the general-purpose approach, the parameters of each cells are those of a lumped-element circuit, and only the cascade of a large number of small sections converges to a good approximation of a transmission line; on the contrary, with the simplified approach, the parameters of each cell and of the cascade are exactly those of transmission lines irrespective of n.

Thus, a value of n in the hundreds can safely handle any practical temperature excursion if the simplified approach is

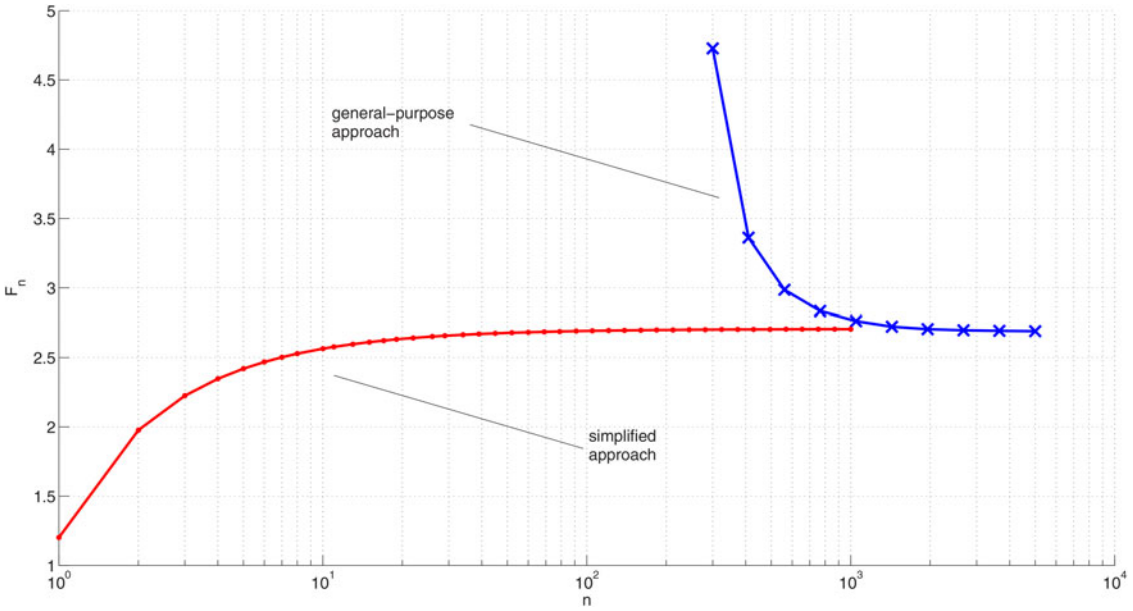

Fig. 3. Comparison between the general-purpose approach Section III and the simplified approach of Section IV in computing the noise factor of an ideal coaxial cable on a fixed source termination.

https://doi.org/10.1017/S1759078715000069 Published online by Cambridge University Press

Table 1. Cable parameters used to generate the results of Fig. 3.

General-purpose approach		Simplified approach	
R	48 mΩ/m	S_{11}	0
L	243 nH/m	S_{12}	$1/\sqrt{2}$
G	10 mS/m	S_{21}	$1/\sqrt{2}$
C	10 pF/m	S_{22}	0
f	10 GHz	Z_c	50 Ω
l	1.41 m	Z_0	50 Ω

used: moreover, this number will only depend on the temperature shape along the cable, but not on its physical length or considered frequency. This is not the case with the general-purpose approach, for which n is typically in the thousands for frequencies of the order of 10 GHz and lengths of the order of 1 m: of course, so large values are enough for any practical temperature shape.

From a practical point of view, Fig. 3 suggests one possible way of setting n that is iteratively increasing the number of cells until the computed value of noise factor saturates to a constant value within a pre-specified absolute or relative error.

V. SIMULATION OF CABLE SMALL-SIGNAL PARAMETERS

As stated above, the approaches presented in Sections III and IV allow us to determine the noise parameters of a transmission line subject to thermal gradients, provided that the temperature shape along the line is known, as well as the dependence of those parameters on temperature – or, more in general, on the longitudinal position. In this section, it will be briefly illustrated how this information can be achieved.

First, the problem of determining the physical temperature at the different sections of the line will be addressed. Unluckily, this is not a trivial task to carry out by direct measurement, due to inaccessibility of some cable portions and in particular of the inner conductor, as well as to the difficulty of a good thermal contact of the diode sensors with the cylindrical outer conductor. As a consequence, only a few points can typically be probed with temperature sensors, while the complete distribution has to be extracted by means of thermal simulations, with specific software (e.g., COMSOL Multiphysics). Furthermore, it is assumed in the following that the temperatures of the two conductors at the end points are approximately equal: if possible, however, this condition should be verified experimentally rather than forced by hypothesis.

Although the mechanisms of heat transfer are rather complex, however, some quite safe assumptions can often come in handy, at least to get a first insight into the problem. In particular, convection is usually negligible in the frame of cryogenic measurements of active devices, since these are carried out under high vacuum levels. Similarly, radiation can often be neglected with respect to conduction, which is the main mechanism involved. Moreover, it can be safely assumed that conduction takes place along the z-axis only; if, however, a good thermal insulator (e.g., Teflon) is used as the dielectric material of the cable under analysis, the thermal shape of the two conductors may differ by a certain amount.

Under these simplified assumptions, the temperature shape along either conductor can be approximately determined by means of the heat equation:

$$q_z = -k(T) \cdot A(z) \cdot \frac{dT}{dz} \tag{27}$$

with appropriate boundary conditions, which may be determined experimentally by directly measuring the conductor physical temperature at its end points. In (27), q_z is the heat flux (W/m^2) in the positive z-direction, $k(T)$ is the thermal conductivity (W/m/K) of the material (not to be confounded with k_i of Section IV), dT/z is the temperature gradient (K/m) and $A(z)$ is the area (m^2) perpendicular to the heat flux direction.

If steady-state conditions are considered and no heat generation (or loss) from the conductor sides takes place, the heat transfer rate q_z must be independent of z. This reasoning applies to any differential element dz as a consequence of the energy conservation requirement, even if the cross-sectional area varies with position, and the thermal conductivity varies with temperature. It is thus convenient to work with Fourier's law, which, expressed in its integral form, reads:

$$q_z \int_{z_1}^{z_2} \frac{dz}{A(z)} = -\int_{T_1}^{T_2} k(T) dT. \tag{28}$$

For either conductor (28) can be applied independently, with the appropriate values of A, which is constant, and of $k(T)$. If the latter is assumed to be constant, (28) simplifies significantly:

$$-k \cdot \Delta T = \frac{q_z}{A} \cdot \Delta z, \tag{29}$$

which implies a linear dependence of T with z. Once $T(z)$ has been determined for both conductors, it must be verified that the two temperatures are actually equal, or at least similar, at every z. If this is the case, the temperature of the cable's dielectric – which has to be featured by a finite, yet good, thermal resistivity – can also be set equal to $T(z)$. Note, indeed, that in both Sections III and IV the case of different temperatures for the two conductors and the dielectric was not addressed: in fact, temperature was considered constant across each cross-section of the distributed line. If this was not the case, the fundamental hypothesis of the proposed approaches would fail, thus jeopardizing the validity of their results.

It is important to stress that the above simplified description of heat exchange in a cable is mainly intended as a help to visualize the basic processes taking place in typical measurement conditions: it is left to the Reader to verify whether (or to what extent) the same simplifying assumptions are legitimate in other cases of their interest, and possibly to devise more complex techniques to determine the dependence of temperature versus z. In this paper, this has been accomplished by means of thermal simulations, under the hypothesis of cables thermally isolated from the environment (i.e., heat exchange through convection and radiation was neglected), but taking into account the non-linear dependence of thermal conductivity on materials and temperature itself.

The remaining part of this section is devoted to discussing how to determine the small-signal parameters of the cable

https://doi.org/10.1017/S1759078715000069 Published online by Cambridge University Press

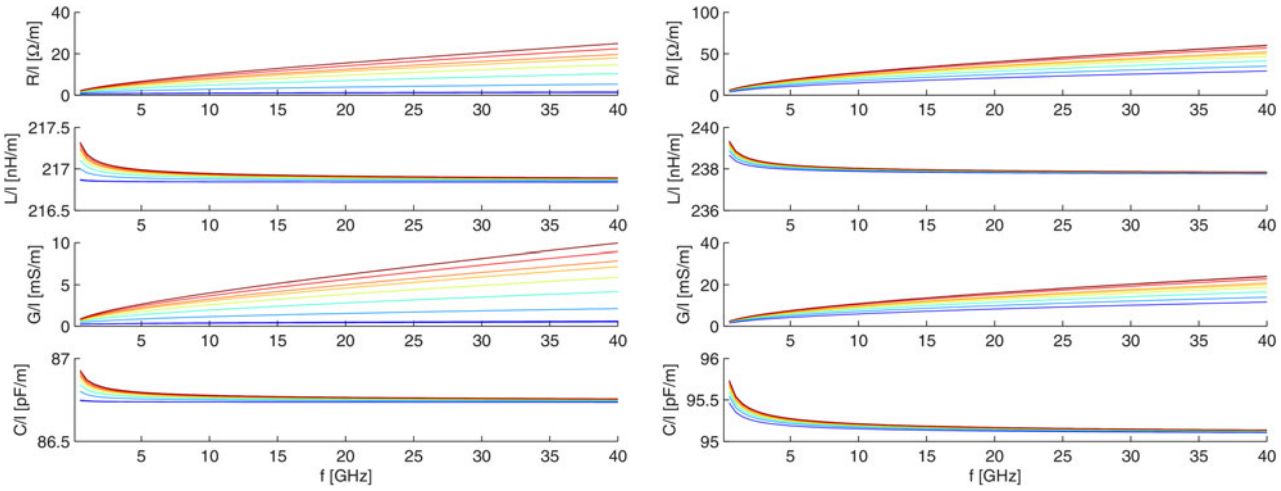

Fig. 4. Computed primary parameters of commercial coaxial cables, for temperatures from 25 K (lowest curves) to 298 K (highest curves). Left: Be–Cu cable. Right: steel cable.

under analysis, and to examining how this allows avoiding the direct simulation of noise parameters under thermal gradients.

Quite trivially, the most immediate way to determine the small-signal parameters of a cable is by three-dimensional (3D) electromagnetic (EM) simulations, which, again, can be performed in advanced environments such as COMSOL Multiphysics, Ansys HFSS, and so on. The key point to focus here is that these simulations need neither to represent the temperature dependence along the z-axis, nor to include the whole cable. On the contrary, constant-temperature simulations of arbitrary lengths of transmission line are of interest. This aspect is not as much an advantage as an inherent feature of the proposed formulation: nevertheless, it does come with advantageous side effects, since it allows reducing computation times by shortening the length of the simulated transmission line.

It is worth noting that closed formulae – which are available for the most common transmission line types – could be used equivalently (i.e., instead of performing EM simulations), as long as they take losses into account: through the possibility of tuning losses, the contribution of temperature can be considered in an indirect fashion.

The second step of this procedure consists in obtaining, for each temperature, the desired primary or secondary line parameters from the corresponding small-signal simulation – or closed-formula computation. The following formulae, for instance, may be used to obtain the characteristic impedance and propagation constant of a transmission line from its scattering matrix and physical length:

$$Z_c = \sqrt{Z_{in,sc} \cdot Z_{in,oc}}, \tag{30}$$

$$\gamma = \frac{1}{l}\operatorname{atanh}\left(\frac{Z_{in,sc}}{Z_c}\right) = \frac{1}{l}\operatorname{atanh}\left(\frac{Z_c}{Z_{in,oc}}\right), \tag{31}$$

where $Z_{in,sc}$ and $Z_{in,oc}$ are the input impedance with the output port short- and open-circuited, respectively. Note that Z_c is in general complex, nevertheless its imaginary part is expected to be negligible in the considered case of a coaxial cable at high frequencies: in fact, it may advisable in some cases to force the condition $\Im\{Z_c\} = 0$ to avoid numerical errors in subsequent calculations. As to γ, note that directly applying (31) to a cable of arbitrary length may yield wrong results, due to line periodicity: nevertheless these effects can be fixed either by unwrapping or, more simply, by simulating short line lengths. The latter solution also comes with reduced simulation times.

To apply the general-purpose approach of Section III, one last step is required, i.e. determining the line primary parameters from Z_c and γ:

$$Z = \gamma \cdot Z_c, \tag{32}$$

$$Y = \frac{\gamma}{Z_c}. \tag{33}$$

As an example, simulated primary parameters of two types of commercial coaxial cables are reported in Fig. 4. It appears clearly how losses are dependent on temperature and cable material; also, it is worth noticing that the reactive parameters are almost constant over temperature, as expected.

From such data, available at discrete frequencies, the behavior of the line primary parameters can be accurately reconstructed as continuous functions of frequency through spline interpolation, and then used for the method described in Section III. The same consideration holds as to the quite simpler task of determining line loss as a function of frequency, which is the only information needed to apply the approach of Section IV.

VI. SUMMARY AND DISCUSSION

The treatment illustrated so far may appear quite fragmented: this is partly due, however, to the fact that the presented approaches and techniques are not totally distinct. On the contrary, they can be combined in a number of ways which it would be pointless to enumerate, and which the interested Reader can easily figure out on their own, as long as the key points have been made clear. This section, therefore, is devoted to exemplify the proposed theory by means of well defined, representative cases.

As a reference for this section, the flow chart of both the general-purpose and simplified approaches (see Sections III

https://doi.org/10.1017/S1759078715000069 Published online by Cambridge University Press

and IV, respectively) is depicted in Fig. 5(a). Indeed, the two approaches follow identical steps, although the relevant information is represented, at certain steps, in different ways. In particular, the transmission-line behaviors are given as primary and secondary parameters, respectively.

In the basic implementation, both approaches require that geometrical and thermal properties of the cable (or transmission line) under analysis be known, as well as the actual temperature at least at its end points. Thus, the temperature shape can be computed or simulated over the whole cable; in addition, the transmission-line parameters at any fixed temperature can be determined. However, a relatively small set of temperatures may be analyzed directly, and interpolation be relied upon to gain a continuous knowledge of line parameters versus temperature.

This information is sufficient, with both approaches, to compute numerically scattering and noise parameters of the cable in an idealized fashion. It is possible, however, to link more directly the results of the simulation to an actual cable specimen, if its *S*-parameters under thermal gradient are known by the measurement: to do so, a variation of the simplified approach can be exploited (dashed arrow in the flow chart).

The core of the theory presented in this work is completely encompassed by the above recapitulation. Nevertheless, the concepts developed to estimate the noise parameters of a cable under thermal gradient also come in handy to fulfill more specific tasks which, in turn, may be ancillary to the original purposes. Thus, the information gathered with the aim of estimating noise parameters can be used to approximate the *S*-parameters under temperature variation from those measured at ambient temperature. This idea is illustrated in Fig. 5(b), which may be regarded as an expansion of the dashed box in Fig. 5(a).

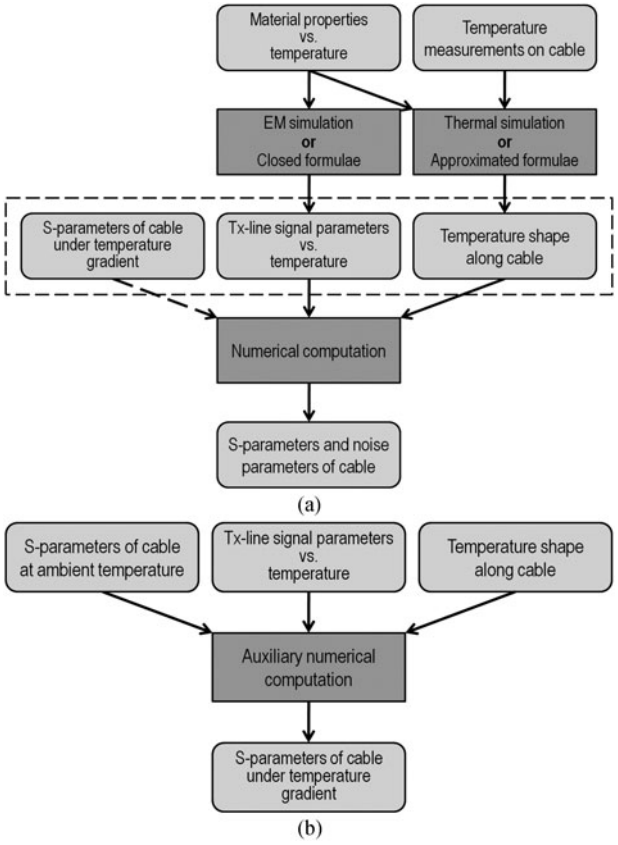

Fig. 5. Flow charts illustrating the steps to apply the proposed numerical approaches. Subfigure (a) provides an overview of the general-purpose and simplified algorithms; the dashed arrow applies optionally, and only in case the simplified algorithm is adopted. The dashed box can be expanded as shown in subfigure (b), in case the technique of Section IV is used to estimate the *S*-parameters of the cable under cryogenic gradient.

VII. EXPERIMENTAL RESULTS

A measurement campaign was purposely undertaken to complement the mathematical formulation above. Experimental results, in agreement with [13], indicate that the proposed approach correctly predicts the noise behavior of coaxial cable subject to thermal gradients. The setup used for measurements consists of a custom cryogenic probe station (depicted in Fig. 6), a vector network analyzer (Anritsu 37397D) for scattering measurements, and a spectrum analyzer (Agilent E4448A) for noise measurements, in conjunction with an Agilent 346C noise source. Pressure and temperature are controlled, respectively, by means of an Alcatel ACS 1000 and a LakeShore 340. A vacuum level of 10^{-7} mbar is obtained through an Alcatel Drytel 1025, while the chamber is cooled by a CryoDyne closed-loop cryostat made of a two-stage cold head and a Helium compressor (8200 CTI-Cryogenics).

In a first attempt [17], the noise figure of the whole chain inside the vacuum chamber was measured, namely of the cascade of the input cables, a pair of radiofrequency probes landing on a coplanar thru, and the output cables. Noise-figure measurements were performed by the *Y*-factor method, basically confirming the validity of the proposed numerical approaches: in particular, the general-purpose method of Section III was used to determine the small-signal and noise parameters of the coaxial cables. Nevertheless, significant measurement uncertainties were experienced, due both to the nature of the device under test and to unavoidable indefiniteness in the description of some blocks in the measurement chain.

Therefore, a second attempt was made to obtain a more reliable validation. This goal was mainly pursued by simplifying as much as possible the setup, and in particular by considering a DUT as similar as possible to what can be actually

Fig. 6. Picture of the custom cryogenic probe station.

https://doi.org/10.1017/S1759078715000069 Published online by Cambridge University Press

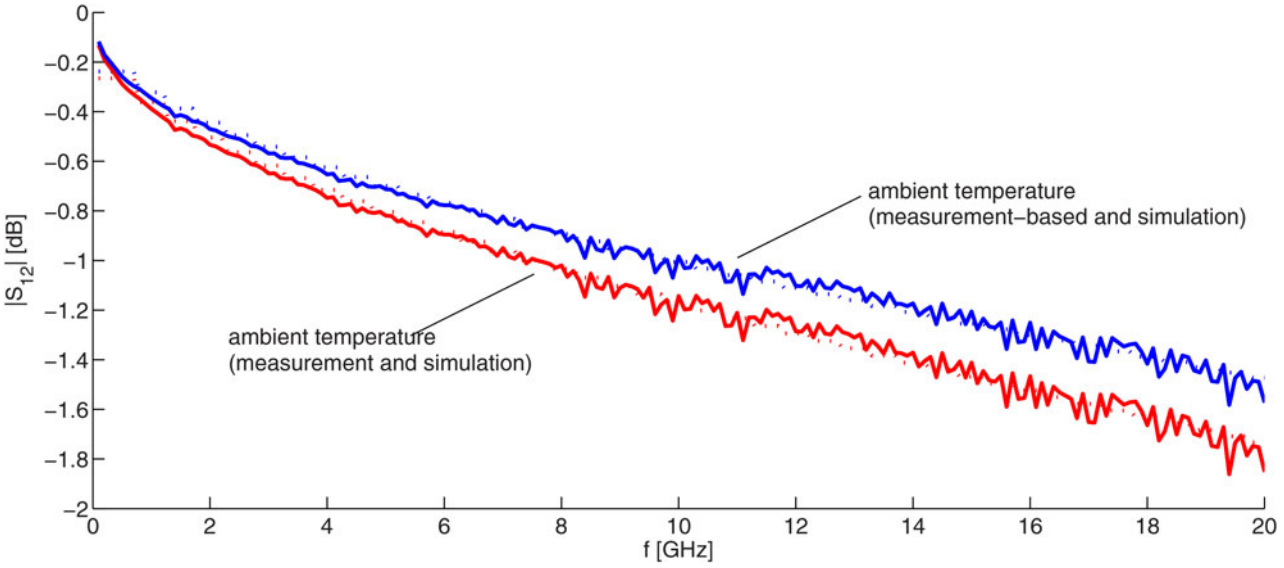

Fig. 7. Comparisons of cable loss at ambient temperature (lower curves) and under a 150°C thermal excursion (higher curves). Dotted curves are completely based on simulations. Of the other two curves, that at ambient temperature is measured, whereas that under thermal gradient is derived from the former based on the approach described in Section IV. Normalization impedance is 50 Ω.

simulated. In this second try, indeed, the pure cascade of a 38-cm copper cable and an 8-cm steel cable was simulated and measured.

As to simulations, these were performed in the COMSOL Multiphysics environment, and yielded the results already presented in Fig. 4. These were first used to approximate the DUT *S*-parameters under a 150°C thermal excursion (from 150 K at the input to 300 K at the output) based on the method of Section V, and then to obtain the cable noise parameters according to the simplified approach of Section IV.

A comparison between measured and simulated loss at ambient temperature is shown in Fig. 7, which also reports loss under the considered thermal gradient, as derived by a direct simulation as well as by adjusting ambient-temperature *S*-parameters (see Section IV and Fig. 5(b)). From the graph a remarkable agreement can be observed at ambient temperature, whereas a direct check was not made in this case as to *S*-parameters under thermal gradient.

Nevertheless, an indirect indication of the correctness of these results can be found in Fig. 8, showing the noise figure of the cable at ambient temperature, as computed by *S*-parameters and physical temperature, and that of the cable under cryogenic conditions, as obtained by direct measurements and simulations.

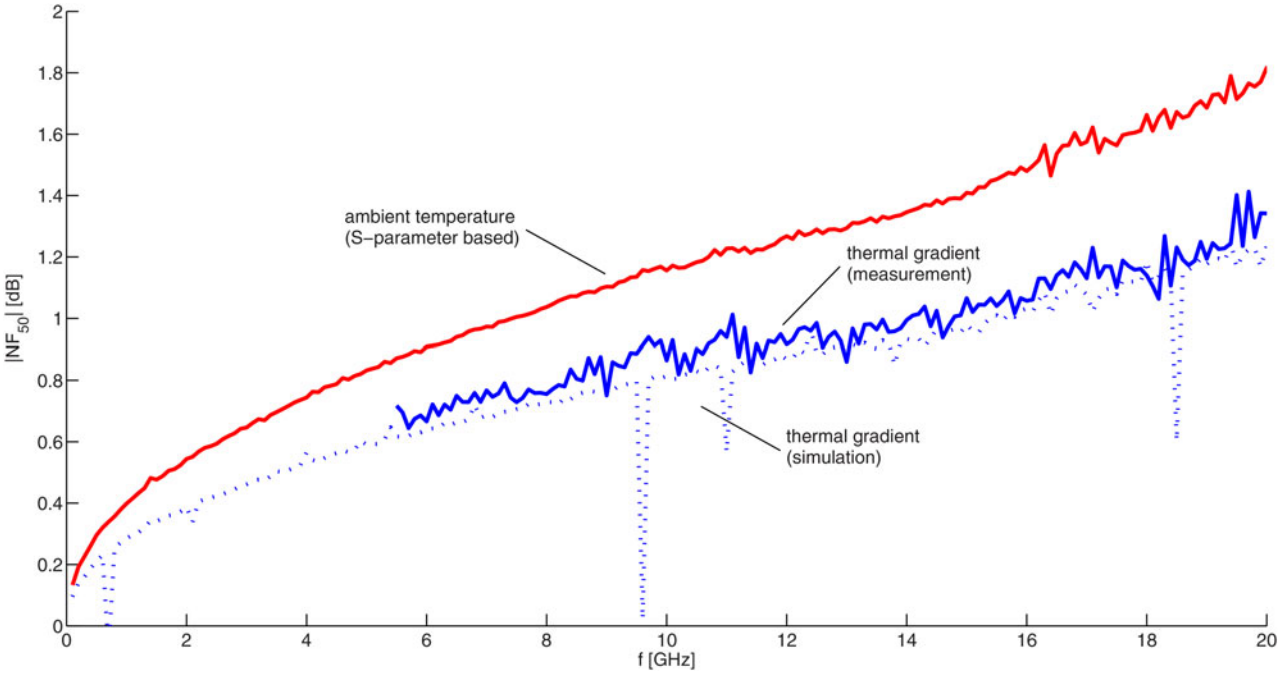

Fig. 8. Comparisons of cable noise figure at ambient temperature and under a 150°C thermal excursion. The ambient-temperature measurement is derived from *S*-parameters. Of the two curves under thermal gradient, the continuous one is obtained by the direct cold-source measurement, whereas the dotted one is derived based with the approach described in Section IV.

https://doi.org/10.1017/S1759078715000069 Published online by Cambridge University Press

In this case, noise measurements were carried out by the cold-source method, since the input end of the cooled cable was inside the vacuum chamber and therefore could not be connected to a diode noise source. In order to minimize the effects of receiver drifts, an electromechanical switch was automatically controlled to allow performing, at each frequency, calibration and measurement readings all in a row. Also, isolators were used ahead of the receiver to avoid errors related to finite bandwidth and source termination changes [12].

Simulations, on the other hand, were based on the simplified approach of Section IV, in the version exploiting cable *S*-parameters (dashed arrow of the flow chart in Fig. 5(a)); moreover, instead of measuring *S*-parameters directly under cryogenic gradient, these were estimated from those at ambient temperature (already shown in Fig. 7).

With a focus on noise figure under thermal gradient, Fig. 8 testifies a substantial agreement between simulated and measured values. It can thus be concluded that the proposed numerical approaches represent viable methods to evaluate both small-signal and noise parameters of coaxial cables; although a more definitive check can be devised requiring the full knowledge, obtained by measurements, of cable noise parameters.

As a last remark, it is worth noting that the dotted trace representing simulated results is featured by undesired outliers at apparently random frequency points. These peaks are mere artifacts related to numerical errors, which arise from elaborating measured *S*-parameters through segmentation into a large number of cells and subsequent reconstruction. Fortunately, however, they can easily be removed, provided that contiguous frequencies have been analyzed.

VIII. CONCLUSION

Several mathematical approaches for numerically evaluating the small-signal and noise parameters of a transmission line under thermal gradients have been presented, which can be useful in fields such as cryogenic noise measurements, analysis of cold and hot noise standards (based on Johnson noise), and whenever a significant temperature excursion takes place in a signal path with specific noise requirements. The proposed formulae are easy to implement and allow handling arbitrary temperature shapes. In particular, a dependence of the electrical parameters on temperature as functions of the longitudinal position is taken into account. The proposed theory has been experimentally tested, and a good agreement has been found between simulations and measurements.

REFERENCES

[1] Schleeh, J.; Rodilla, H.; Wadefalk, N.; Nilsson, P.; Grahn, J.: Characterization and modeling of cryogenic ultralow-noise InP HEMTs. IEEE Trans. Electron Devices, **60** (1) (2013), 206–212. DOI: 10.1109/ted.2012.2227485.

[2] Samoska, L. et al.: W-band cryogenic InP MMIC LNAs with noise below 30 K, in 2012 IEEE MTT-S Int. Microwave Symp. Digest (MTT), 2012, 1–3. DOI: 10.1109/mwsym.2012.6258356.

[3] Bryerton, E.W.; Morgan, M.; Pospieszalski, M.W.: Ultra low noise cryogenic amplifiers for radio astronomy, in 2013 IEEE Radio and Wireless Symp. (RWS), 2013, 358–360. DOI: 10.1109/rws.2013.6486740.

[4] Klauda, M. et al.: Superconductors and cryogenics for future communication systems. IEEE Trans. Microw. Theory Tech., **48** (7) (2000), 1227–1239. DOI: 10.1109/22.853466.

[5] Narahashi, S.; Satoh, K.; Kawai, K.; Koizumi, D.: Cryogenic receiver front-end for mobile base stations, in 2008 China-Japan Joint Microwave Conference, 2008, 619–622. DOI: 10.1109/cjmw.2008.4772507.

[6] Colangeli, S.; Ciccognani, W.; Palomba, M.; Limiti, E.: Automated extraction of device noise parameters based on multi-frequency, source-pull data. Int. J. Microw. Wirel. Technol., **6** (1) (special issue), Feb. (2014), 63–72. DOI: 10.1017/S1759078713000822.

[7] Wiatr, W.: Comments on "Cryogenic noise parameter measurements of microwave devices". IEEE Trans. Instrum. Meas., **53** (2) (2004), 619. DOI: 10.1109/tim.2004.823649.

[8] Rolfes, I.; Musch, T.; Schiek, B.: Cryogenic noise parameter measurements of microwave devices. IEEE Trans. Instrum. Meas., **50** (2) (2001), 373–376. DOI: 10.1109/19.918145.

[9] Wait, D.F.: Measurement accuracies for various techniques for measuring amplifier noise, in 39th ARFTG Conf. Digest-Spring, vol. 21, 1992, 43–52. DOI: 10.1109/arftg.1992.326971.

[10] Pospieszalski, M.W.: Modeling of noise parameters of MESFETs and MODFETs and their frequency and temperature dependence. IEEE Trans. Microw. Theory Tech., **37** (9) (1989), 1340–1350. DOI: 10.1109/22.32217.

[11] Lane, R.Q.: The determination of device noise parameters. Proc. IEEE, **57** (8) (1969), 1461–1462. DOI: 10.1109/proc.1969.7311.

[12] Limiti, E.; Ciccognani, W.; Colangeli, S.: Characterization and modeling of high-frequency active devices, in Microwave De-embedding – from Theory to Applications, chapter 3. G. Crupi and D. Schreurs (Eds.) Oxford (The Boulevard, Langford Lane, kidlington, Oxford OX5 1GB, UK) 2013, 97–150.

[13] Delcourt, S. et al.: On-wafer high frequency noise power measurements under cryogenic conditions: a new de-embedding approach, in 2004. 34th Eur. Microwave Conf., vol. 2, 2004, 913–916.

[14] Stelzried, C.T.: Microwave thermal noise standards. IEEE Trans. Microw. Theory Tech., **16** (9) (1968), 646–655. DOI: 10.1109/tmtt.1968.1126767.

[15] Hillbrand, H.; Russer, P.: An efficient method for computer aided noise analysis of linear amplifier networks. IEEE Trans. Circuits Syst., **23** (4) (1976), 235–238. DOI: 10.1109/tcs.1976.1084200.

[16] Hillbrand, H.; Russer, P.: Correction to "An efficient method for computer aided noise analysis of linear amplifier networks". IEEE Trans. Circuits Syst., **23** (11) (1976), 691–691. DOI: 10.1109/tcs.1976.1084145.

[17] Colangeli, S.: Numerical evaluation of cable noise parameters under cryogenic thermal gradients, in EuMIC, 2014.

Sergio Colangeli was born in Roma, Italy, in 1984. He received the M.S. degree in Electronic Engineering in 2008 from the University of Roma "Tor Vergata," as well as the Ph.D. degree in Telecommunications and Microelectronics in 2013. He has been with the Electronics Department of that University ever since, currently holding a research grant. His research interests include low-noise design methodologies for microwave applications, with particular reference to low-noise amplification, and small-

https://doi.org/10.1017/S1759078715000069 Published online by Cambridge University Press

signal and noise characterization and modeling of microwave active devices. Dr. Colangeli was a recipient of the EuMIC Young Engineer Prize in 2012.

Riccardo Cleriti was born in Frascati, Italy, in 1985. He received the M.S. degree in Electronic Engineering in 2011 from the University of Roma "Tor Vergata." In the same university he has attended a Ph.D. course in Telecommunications and Microelectronics, and is going to defend his dissertation in a few months. His work has focused on cryogenic characterization and small-signal and noise modeling of microwave active devices, and submillimeter low-noise amplification; he is also currently involved in a European project whose goal is to design a submillimeter passive/active body scanner for security applications.

Walter Ciccognani was born in Roma, Italy, in 1977. He received the M.S. degree in Electronic Engineering in 2002 and the Ph.D. degree in Telecommunications and Microelectronics (in 2007) both conferred by the University of Roma "Tor Vergata" where he is an assistant professor since 2012 and where he has been teaching the course in microwave measurements since 2013. He has coauthored over 60 papers in international scientific journals and conferences and has been involved in several national and international research projects, in those contexts he had the opportunity to collaborate with the major European semiconductor foundries. His main interests include linear microwave circuit-design methodologies, linear and noise analysis/measurement techniques, and small-signal and noise modeling of microwave active devices.

Ernesto Limiti has been a full professor of Electronics in the Electronic Engineering Department of the University of Roma "Tor Vergata" since 2002. His research activities are focused on three lines, all in microwave and millimeter-wave electronics. The first concerns active devices oriented to small-signal, noise, and large-signal modelings. Novel methodologies are developed for noise characterization and modeling; equivalent-circuit modeling strategies are implemented both for small- and large-signal operating regimes for GaAs, GaN, SiC, Si, and InP MESFET/HEMT devices. The second line is related to design methodologies and characterization methods for low-noise devices and circuits. His main focus is on extremely low-noise cryogenic amplifiers. His collaborations run with major radio astronomy institutes in Europe (FP6 and FP7 projects). The third line is analysis and design methodologies for linear and non-linear microwave circuits. He is a referee of several international microwave and millimeter-wave electronics journals and is a member of several international conference and workshop steering committees.

https://doi.org/10.1017/S1759078715000069 Published online by Cambridge University Press